haematologica
Journal of the Ferrata Storti Foundation

Sustained molecular clearance of the *MYD88* p.L265P-mutant clone preceding resolution of cold agglutinin syndrome after autologous stem cell transplantation

by Kazuaki Yokoama, Nozomi Yusa, Koji Jimbo, Atsuko Takahashi, Kazuo Ogami, Eigo Shimizu, Seiya Imoto, Tokiko Nagamura-Inoue and Yasuhito Nannya

Received: February 17, 2026.
Accepted: May 26, 2026.

Citation: Kazuaki Yokoama, Nozomi Yusa, Koji Jimbo, Atsuko Takahashi, Kazuo Ogami, Eigo Shimizu, Seiya Imoto, Tokiko Nagamura-Inoue and Yasuhito Nannya. Sustained molecular clearance of the MYD88 p.L265P-mutant clone preceding resolution of cold agglutinin syndrome after autologous stem cell transplantation.
Haematologica. 2026 June 4. doi: 10.3324/haematol.2026.300719 [Epub ahead of print]

Sustained molecular clearance of the *MYD88* p.L265P-mutant clone preceding resolution of cold agglutinin syndrome after autologous stem cell transplantation

Kazuaki Yokoyama[1,2], Nozomi Yusa[3], Koji Jimbo[4], Atsuko Takahashi[2], Kazuo Ogami[2], Eigo Shimizu[5], Seiya Imoto[5], Tokiko Nagamura-Inoue[2], and Yasuhito Nannya[1,4]

[1]Department of Hematology/Oncology, Research Hospital, The Institute of Medical Science, The University of Tokyo, Tokyo, Japan

[2]Department of Cell Processing and Transfusion, Research Hospital, The Institute of Medical Science, The University of Tokyo, Tokyo, Japan

[3]Department of Laboratory Medicine, Research Hospital, The Institute of Medical Science, The University of Tokyo, Tokyo, Japan

[4]Division of Hematopoietic Disease Control, The Institute of Medical Science, The University of Tokyo, Tokyo, Japan

[5]Division of Health Medical Intelligence, Human Genome Center, The Institute of Medical Science, The University of Tokyo, Japan

Corresponding author: Kazuaki Yokoyama, M.D., Ph.D.,

Department of Hematology/Oncology,

The Institute of Medical Science, The University of Tokyo,

4-6-1 Shirokanedai, Minato-ku, Tokyo 108-8639, Japan. Tel: +81-3-3443-8111, Fax: +81-3-5449-5429, E-mail: k-yoko@ims.u-tokyo.ac.jp

Running title
MYD88-mutant clone clearance preceding CAS resolution post-ASCT

Text word count: 1,450;

Number of tables: 1;

Number of figures: 2

Keywords: cold agglutinin syndrome, *MYD88*, circulating tumor DNA, autologous stem cell transplantation

AUTHOR CONTRIBUTIONS

Conception and design: K.Y., Y.N.; Administrative support: Not applicable; Provision of study materials or patients: J.K., A.T., K.O., T.N-I.; Collection and assembly of data: K.Y., N.Y., E.S., S.I.; Data analysis and interpretation: K.Y., Y.N.; Manuscript writing: K.Y., Y.N.; Final approval of manuscript: All authors; Accountable for all aspects of the work: All authors

DATA-SHARING STATEMENT

All available data are presented in the text and figures of this case report. Additional requests for information can be made to the corresponding author.

DISCLOSURES

K.Y. received lecture fees from AstraZeneca Co. and Otsuka Pharmaceutical Co., Ltd.; K.Y. is an outside director of Liquid Mine Co. and received research funding from Nippon Shinyaku and Liquid Mine Co.; S.I. received honoraria from Daiichi Sankyo RD Novaré, BrightPath Biotherapeutics Co. Ltd., and Liquid Mine Co.; Y.N. received lecture fees from Novartis Pharma Co. Ltd. The remaining authors have no conflicts of interest to declare.

Cold agglutinin disease (CAD) is a rare autoimmune hemolytic anemia mediated by IgM autoantibodies causing red blood cell agglutination <37°C.[1] Cold agglutinin syndrome (CAS) occurs in B-cell lymphoproliferative disorders and is pathophysiologically distinct from cold agglutinin disease (CAD).[1] Autologous stem cell transplantation (ASCT) is a standard consolidation treatment for chemotherapy-sensitive relapsed diffuse large B-cell lymphoma (DLBCL). However, its application in CAS-complicated cases remains challenging because of the risk of temperature-dependent agglutination during apheresis and infusion.[2,3] Only five ASCT cases in patients with CAD/CAS have been reported,[2,4-7] with only one case achieving complete remission in the cold agglutinin (CA) titer.[6] Whether ASCT can cure CAS and its underlying mechanisms remain unknown. Herein, we present a case of *MYD88* p.L265P-mutated splenic marginal zone lymphoma (SMZL) with CAS that transformed into DLBCL and was successfully treated with ASCT.

This study followed the Declaration of Helsinki and was approved by the Institutional Review Board of the Institute of Medical Science, University of Tokyo (approval numbers: 26-112-270402; 2020-1-0422; 2024-103-0326). Cell-free DNA and genomic DNA were extracted using the Maxwell RSC ccfDNA Plasma Kit (Promega) and Gentra Puregene Blood kit (Qiagen). For targeted deep sequencing, libraries were prepared using the TruSight Myeloid Panel (Illumina). For whole-genome sequencing (WGS), libraries were prepared using TruSeq Nano DNA Library Prep kit and sequenced on NovaSeq 6000. The Genomon 2.6.2 pipeline identified somatic single nucleotide variants (SNVs) and structural variants (SVs) (https://genomon.readthedocs.io/ja/latest/); Control-FREEC estimated copy number alterations (CNAs) and tumor purity (https://github.com/BoevaLab/FREEC). Clonal architecture was inferred using PyClone-VI, integrating variant allele frequencies (VAFs) of SNVs and SVs with CNA profiles (https://github.com/Roth-Lab/pyclone-vi). Cancer cell

fractions (CCF), defined as the fraction of cancer cells carrying each mutation, corrected for CNAs and tumor purity, were estimated for each cluster. Phylogenetic trees were constructed using the pigeonhole principle.[8] Circulating tumor DNA (ctDNA) was quantified using digital PCR targeting *MYD88* p.L265P (QX200, Bio-Rad).

A 48-year-old woman presented with severe anemia, jaundice, and massive splenomegaly in October 2015. Laboratory findings revealed hemolytic anemia with a cold agglutinin (CA) titer of 1:1024, positive direct agglutination test, and negative direct antiglobulin test for IgG. Serum haptoglobin was decreased (2 mg/dL; normal 19–170) with elevated lactate dehydrogenase (LDH; 450 U/L; normal 124–222) showing an LDH1-predominant isozyme pattern (37.3%; normal 20–31) consistent with hemolysis. Serum immunofixation detected an IgM-κ monoclonal protein with elevated free κ light chain (314 mg/L; normal 3.3–19.4) and κ/λ ratio of 10.43 (normal 0.26–1.65). Serum IgM level was within normal range (180 mg/dL; normal 35–220). Soluble IL-2 receptor (sIL-2R) level was elevated at 3320 U/mL. Pathological examination of the extracted spleen confirmed SMZL. Targeted deep sequencing detected *MYD88* p.L265P (VAF 14.6% in the spleen [SP] and 18.4% in the bone marrow [BM]), which was identified in serum ctDNA (VAF 3.2%), supporting lymphoma-associated CAS. Following splenectomy, hemolysis improved with normalization of haptoglobin (35 mg/dL) as ctDNA decreased to 1.0%, despite persistently high CA titers (1:512–1:2048; Figure 1A). Eight cycles of rituximab achieved BM *MYD88* p.L265P -VAF reduction to 0.4% with sIL-2R normalization, though CA titers remained elevated (Figure 1A).

In August 2021, ctDNA levels increased to 7.6%, preceding the clinical progression of lymphoma by three months (Figure 1A). In November 2021, the patient developed cervical lymphadenopathy and was diagnosed with transformed DLBCL (activated B-cell type) by

histological examination of the cervical lymph nodes. Serum free light chain analysis at relapse showed κ elevation (κ 58.8 mg/L, λ 8.5 mg/L, κ/λ ratio 5.92) with immunofixation-positive IgM-κ M-protein. Following one cycle of R-CHOP and three cycles of bendamustine and rituximab, the patient achieved a complete metabolic response on positron emission tomography–computed tomography and negative conversion of ctDNA. Considering her young age and chemotherapy-sensitive disease status, ASCT was planned as consolidation therapy for transformed DLBCL. Notably, the indication for ASCT was lymphoma control rather than CAS management, as active hemolysis had not recurred following splenectomy.

To define clonal relationships, we performed WGS of the SP and lymph node (LN) at relapse (average depth: SP; 32.3×, LN; 84.7×, and buccal swab; 33.6×). Across all specimens, 174,490 somatic variants were identified, of which 8,968 (5.1%) shared a common origin. Clonal decomposition identified 10 distinct clonal clusters, with median CCFs ranging from 10.1 – 100.0%. Phylogenetic inference revealed a founder clone (C6; CCF: SP; 80.4%, LN; 100.0%, n=1,398) harboring the pathogenic *MYD88* p.L265P. Three evolutionary branches emerged: (1) an LN-specific transformation-associated branch acquiring *ROBO2*, *EP300*, and *KLF2* mutations and (2) a branch (C5; *BCL10* p.L163X) diverging into SP-specific (C4/C0) and shared (C2/C3; *IGH::PAX5*) sub-branches. All malignant cells remained anchored to the founding *MYD88* p.L265P-mutant trunk.

Mobilization was performed using cyclophosphamide, cytarabine, dexamethasone, etoposide, rituximab (CHASER) chemotherapy, followed by granulocyte colony-stimulating factor and plerixafor. Compared with most reported cases,[2,4-6] prophylactic plasma exchange (PE) was not performed (Table 1) because the patient experienced no clinical hemolysis after splenectomy despite persistently high CA titers. Temperature management during apheresis was achieved using only a blood warmer (36°C) on the return line. Collection over two days

yielded 2.78×10^6 CD34+ cells/kg without complications. The product was cryopreserved without previous washing using ABO-compatible fresh-frozen plasma with 10% dimethyl sulfoxide. Post-thaw viability was excellent (88.4–93.7%), with no visible agglutination before cryopreservation.

High-dose conditioning with cyclophosphamide, etoposide, melphalan, and dexamethasone was administered before ASCT. During stem cell infusion, massive agglutination occurred within minutes of thawing, causing repeated filter occlusion requiring 10 circuit changes over 2 h (Figure 1B-E). Besides transient oxygen desaturation, no severe adverse events occurred and the entire cell dose was successfully infused. Neutrophil engraftment occurred on day +10 and platelet engraftment on day +17. At 3 months post-ASCT, serum immunofixation showed no detectable M-protein with normalization of free light chain levels (κ <0.5 mg/L, λ <0.8 mg/L). Importantly, CA titers progressively declined from 1:1024 at transplantation to complete normalization (<1:64) at 14 months post-ASCT, which was maintained for >30 months (Figure 1A), followed by sustained ctDNA negativity for *MYD88* p.L265P. The patient remained in sustained complete remission of DLBCL and CAS at the last follow-up.

Here, we report a case of *MYD88* p.L265P–mutated SMZL transformed into DLBCL with a high-titer CAS (1:1024), in which ASCT led to sustained remission in both conditions. This case illustrates three key observations relevant to lymphoma-associated CAS management. First, complete normalization of CA titers was achieved post-ASCT, representing a rare and second most reported outcome in the literature. Second, the CA titers did not parallel the molecular kinetics of *MYD88* p.L265P in real time. Finally, high CA titers pose a significant technical risk of agglutination during stem cell infusion, despite the absence of active clinical hemolysis.

Previous reports have suggested that CA titers track lymphoma activity, with CAS often preceding lymphoma diagnosis or accompanying aggressive disease courses.[9,10] In our case, the CA titers did not parallel the ctDNA kinetics of *MYD88* p.L265P. Despite a marked decline in ctDNA levels following splenectomy and rituximab-based therapy, CA titers have remained elevated for years. Considering the short half-life of circulating IgM (5–10 days),[11] this persistence reflects continued CA production by long-term, chemo-insensitive plasma cells[12] that may be outside the *MYD88*-mutant clonal hierarchy yet depend on the lymphoma-associated microenvironment for survival. Complete CA normalization occurred only after sustained molecular remission post-ASCT, suggesting that the CA-producing population ultimately depended on the lymphoma clone or its associated microenvironment.[13] Clinically, persistent CA titers after apparent molecular remission should not be interpreted as evidence of refractory lymphoma.[14,15]

Although splenectomy is considered ineffective in CAD in which hemolysis occurs predominantly through hepatic C3b-mediated clearance,[1,14] our patient's improvement likely resulted from tumor debulking (confirmed by ctDNA reduction), removal of a major site of extravascular hemolysis, and cold avoidance limiting in vivo antibody binding.[1,14] The negative direct antiglobulin test for IgG argues against a significant warm autoimmune component to the hemolysis.

Regarding transplantation management, although prophylactic PE was omitted because of the absence of clinical hemolysis after splenectomy, massive agglutination occurred during stem cell infusion, possibly owing to residual high-titer CA within the cryopreserved product.[3] Among five previously reported CAS/CAD-associated ASCT cases (Table 1),[2,4-7] most employed extensive preventive measures, including PE, and only one achieved complete CA normalization.[7] Our case demonstrates delayed yet durable CA

normalization occurring 13 months after confirmed molecular clearance, with sustained serologic remission for more than 30 months at last follow-up. Retrospectively, preventive measures, such as pre-apheresis PE[2,4-7] or warm saline washing of the apheresis product,[7] may warrant consideration in high-titer CAS to mitigate infusion-related complications.

Overall, this case provides molecular evidence that durable remission of CAS is achievable post-ASCT. *MYD88* p.L265P serves as a valuable traceable biomarker for disease activity, with sustained ctDNA negativity preceding eventual CA normalization. Although ASCT should not be precluded by high CA titers in eligible patients with CAS, meticulous preparation for infusion-related agglutination remains essential.

REFERENCES

1. Berentsen S. How I manage patients with cold agglutinin disease. Br J Haematol. 2018;181(3):320-330.

2. Thompson TZ, Krull AA, Strasburg DJ, Adamski J, Jacob EK, DiGuardo MA. Collection and processing of hematopoietic progenitor cell products at risk of presenting with cold agglutination. Cytotherapy. 2023;25(7):699-703.

3. Krull A, Thompson T, Strasburg D, DiGuardo M, Jacob EK. How do I warm HPC(A) products to maximize cell viability in the setting of cold agglutinin disease? Transfusion. 2022;62(10):1942-1947.

4. Badami KG, Smith MP, Murton D, Rodger S, Atkinson G. Autologous peripheral blood stem cell harvest and transplant in a patient with cold agglutinin disease secondary to lymphoma. Transfus Med. 2017;27(3):222-224.

5. Castonguay M, Bernard L, Corriveau M, et al. Approach to autologous stem cell transplantation in a patient with severe cold agglutinin disease, a case report. Transfusion. 2025;65(3):637-642.

6. Morigi A, Beatrice C, Lisa A, et al. Successful stem cell harvest and autologous transplantation in a patient with cold agglutinin syndrome and aggressive lymphoma. Leuk Lymphoma. 2021;62(4):1007-1009.

7. Crowther H, Collins D, Antonenas V, et al. Successful autologous peripheral blood stem cell harvest and transplant in a patient with cold agglutinins. Bone Marrow Transplant. 2006;37(3):329-330.

8. Nik-Zainal S, Van Loo P, Wedge DC, et al. The life history of 21 breast cancers. Cell. 2012;149(5):994-1007.

9. Döngelli H, Özsan GH. Cold agglutinin syndrome as a precursor for the diagnosis of low-grade lymphoma: a case report. Med Int (Lond). 2025;5(2):12.

10. Yamashita T, Ishida M, Moro H, et al. Primary bone marrow diffuse large B-cell lymphoma accompanying cold agglutinin disease: A case report with review of the literature. Oncol Lett. 2014;7(1):79-81.

11. Schroeder HW Jr, Cavacini L. Structure and function of immunoglobulins. J Allergy Clin Immunol. 2010;125(2 Suppl 2):S41-52.

12. Berentsen S, Barcellini W, D'Sa S, et al. Cold agglutinin disease revisited: a multinational, observational study of 232 patients. Blood. 2020;136(4):480-488.

13. Alexander T, Farge D, Badoglio M, Lindsay JO, Muraro PA, Snowden JA. Hematopoietic stem cell therapy for autoimmune diseases - Clinical experience and mechanisms. J Autoimmun. 2018;92:35-46.

14. Berentsen S, Ulvestad E, Langholm R, et al. Primary chronic cold agglutinin disease: a population based clinical study of 86 patients. Haematologica. 2006;91(4):460-466.

15. Hiepe F, Dörner T, Hauser AE, Hoyer BF, Mei H, Radbruch A. Long-lived autoreactive plasma cells drive persistent autoimmune inflammation. Nat Rev Rheumatol. 2011;7(3):170-178.

Table 1. Clinical characteristics, peri-transplant management, and outcomes of reported cases of autologous stem cell transplantation in cold agglutinin syndrome

Reference (first author, year)	**Crowther et al. (2006)[7]**	**Badami et al. (2017)[4]**	**Morigi et al. (2021)[6]**	**Thompson et al. (2023)[2]**	**Castonguay et al. (2025)[5]**	**Present case**
Underlying disease	Relapsed DLBCL with CAS	MZL with CAS	Relapsed DLBCL with CAS	Plasmacytoma and AL chain / primary amyloidosis with CAS	CAD → DLBCL with CAS → DLBCL with CAS (Relapse)	SMZL with CAS → DLBCL transformation with CAS (Relapse)
Age/Sex	62 M	61 F	56 F	62 M	61 M	48 F
CA titer	1:512 (RT)	1:64 (4°C)	1:256 (4°C)	>1:512 (4°C)	1:4096 (4°C) 1:128 (37°C)	1:1024 (4°C)
Clinical hemolysis present	No	Yes	Yes (resolved)	No	Yes (transfusion-dependent)	Yes (resolved post-splenectomy)
***MYD88* p.L265P mutation**	NA	NA	NA	NA	NA	**Positive**
Splenectomy	Post-ASCT	No	No	No	No	**Yes (pre-ASCT)**
Pre-harvest plasma exchange performed	Yes (×1)	Yes (×2)	Yes (×1)	Yes (×1)	Yes (×5)	**No**
Thermal management / product handling	Room 30°C; warming blanket; return line warmer; 37°C-controlled product warming; warm saline washing	Room 28°C; warming blanket; inlet/return line warmers; 37°C-controlled product warming; no washing	Room >30°C; no line warmer; no product warming; no washing	Room 24°C; warming blanket; inlet/return line warmers; 37°C-controlled product warming; no washing	Room 30°C; warming blanket; return line warmer; 37°C-controlled product warming; no washing	Standard room temperature; return line warmer; no product warming; no washing
Infusion-related complications	None	None	None	None	None	**Massive agglutination, 10 circuit changes**
Engraftment (neutrophils /platelets)	Day +14 / +28	Day +16 / +38	Day +20 / +25	Day +21 / +18	Engrafted	Day +10 / +17
Lymphoma treatment response	CR (15 months)	Relapsed	CR maintained	NA	CR (12 months)	**CR (43 months)**
CA titer normalization	NA	No	Yes	NA	No	**Yes (13 months after mCR; sustained >30 months)**

Bold text highlights features that distinguish the present case, including the longest documented follow-up with sustained lymphoma remission and cold agglutinin normalization. **Abbreviations:** AL, amyloid light chain; ASCT, autologous stem cell transplantation; CA, cold agglutinin; CAD, cold agglutinin disease; CAS, cold agglutinin syndrome; CR, complete remission; mCR, molecular complete remission; DLBCL, diffuse large B-cell lymphoma; MZL, marginal zone lymphoma; NA, not available or applicable; RT, room temperature; SMZL, splenic marginal zone lymphoma.

Figure legends

Figure 1. Clinical course, molecular monitoring, and macroscopic findings during autologous stem cell transplantation for *MYD88*-mutated SMZL with cold agglutinin syndrome. (A) Longitudinal clinical course shows temporal changes in hemoglobin (Hb, red circles), lactate dehydrogenase (LDH, purple triangles, ×100 U/L scale), cold agglutinin (CA) titer (blue squares, logarithmic scale), and *MYD88* p.L265P variant allele frequency (VAF) in bone marrow (BM, brown squares) and circulating tumor DNA (ctDNA, orange diamonds). Horizontal dotted lines indicate the upper limit of normal for CA titer (64×, blue) and LDH (222 U/L, purple). Gray shading denotes treatment periods; vertical dashed lines mark key interventions. Upon diagnosis, ctDNA VAF was 3.2% with CA titer 1024× and elevated LDH (450 U/L). Following splenectomy, Hb improved and ctDNA declined to 1.0% despite persistent high CA titers. Rituximab reduced BM VAF to 0.4% with Hb stabilization and LDH normalization, but CA titers remained elevated (512–1024×). In August 2021, ctDNA increased to 7.6%, preceding clinical relapse by three months. At DLBCL transformation, LDH peaked at 1102 U/L. After salvage chemotherapy and autologous PBSCT, ctDNA (0%), CA titer (<64×), and LDH all normalized, paralleling sustained Hb improvement and demonstrating complete molecular and serological remission maintained for >3 years. (B–E) Macroscopic agglutination during autologous PBSC infusion. (B) Cryopreservation bag immediately post-thaw shows dense white cellular aggregates accumulating at the top of the product. (C) Same bag at 10 min post-thaw; agglutinated material has sedimented near the outlet port. (D) Filter obstruction during infusion. Left: sticky cellular aggregates adhering to the 40-μm filter mesh; progressive accumulation of such material led to repeated filter occlusion. Right: cellular aggregates visible in the downstream infusion line. Ten circuit changes were required during the 2-h infusion. (E) Physical characteristics of the agglutinated

product removed from the occluded filter: cohesive clumps in a petri dish (top) and gel-like material maintaining structural integrity when lifted (bottom), illustrating the severity of cold agglutinin-mediated cellular clumping. This progressive agglutination occurred despite maintaining the product at 36°C.

Figure 2. Clonal architecture and phylogenetic analysis of SMZL-to-DLBCL transformation. (A) Rank plots of corrected variant allele frequency (corrected VAF) demonstrate clonal relationships between SMZL (spleen, SP; upper panel) and transformed DLBCL (lymph node, LN; lower panel). Somatic single nucleotide variants (SNVs) and structural variants (SVs) are ranked in descending order of corrected VAF (local copy number [CNV]- and tumor purity-adjusted VAF). Shared variants (blue, detected in both samples) are prioritized over private variants (green for SP; red for LN). Key driver mutations are annotated: *MYD88* p.L265P, *BCL10* p.L163X, *IGH::PAX5* are shared between compartments, confirming a common clonal origin. Transformation-associated mutations, including *ROBO2* p.R99H, *EP300* p.D1373N, and *KLF2* p.T284I, are exclusively LN-private. The dramatically extended tail in the LN plot (>150,000 variants) reflects the exceptionally high mutation burden within subclone C7, consistent with ongoing genomic instability during transformation. (B) Clonal phylogeny reconstructed from PyClone-VI cancer cell fraction (CCF) estimates using the pigeonhole principle. Nodes represent clonal clusters; edges indicate ancestral relationships. The tree originates from germline (GL). Node colors denote clone patterns; red (SP-specific), blue (LN-specific), orange (decreasing CCF from SP to LN), purple (increasing CCF), and green (stable). Adjacent bar plots show CCF in spleen (red) and lymph node (blue). The founding clone C6 harbors *MYD88* p.L265P (n=1,398 mutations) and anchors all subsequent evolution. Three major branches emerge; (1) an LN-specific transformation-associated branch (C9→C8→C7→C1) sequentially acquiring

ROBO2, EP300, and *KLF2* mutations, with C7 showing exceptionally high mutation burden (n=101,777) and (2) a *BCL10*-mutant branch (C5) diverging into SP-specific (C4→C0) and shared (C2→C3) sub-branches, the latter harboring *IGH::PAX5*. Numbers along branches indicate private mutations acquired at each node.

Figure 1.

A

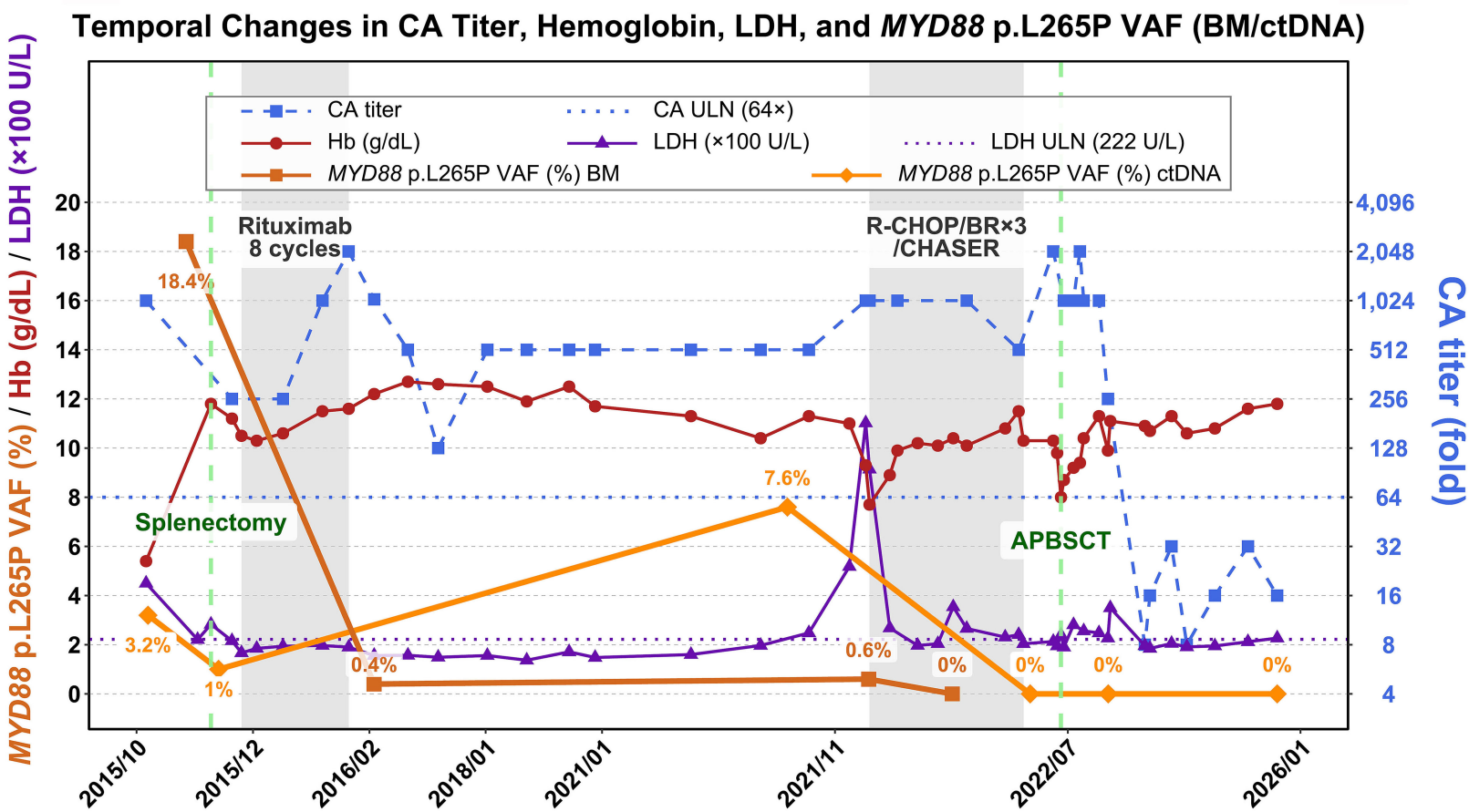
Temporal Changes in CA Titer, Hemoglobin, LDH, and MYD88 p.L265P VAF (BM/ctDNA)
CA titer
CA ULN (64×)
Hb (g/dL)
LDH (×100 U/L)
LDH ULN (222 U/L)
MYD88 p.L265P VAF (%) BM
MYD88 p.L265P VAF (%) ctDNA
Rituximab 8 cycles
R-CHOP/BR×3 /CHASER
Splenectomy
APBSCT
18.4%
3.2%
1%
0.4%
7.6%
0.6%
0%
0%
0%
0%
MYD88 p.L265P VAF (%) / Hb (g/dL) / LDH (×100 U/L)
CA titer (fold)
20
18
16
14
12
10
8
6
4
2
0
4,096
2,048
1,024
512
256
128
64
32
16
8
4
2015/10
2015/12
2016/02
2018/01
2021/01
2021/11
2022/07
2026/01

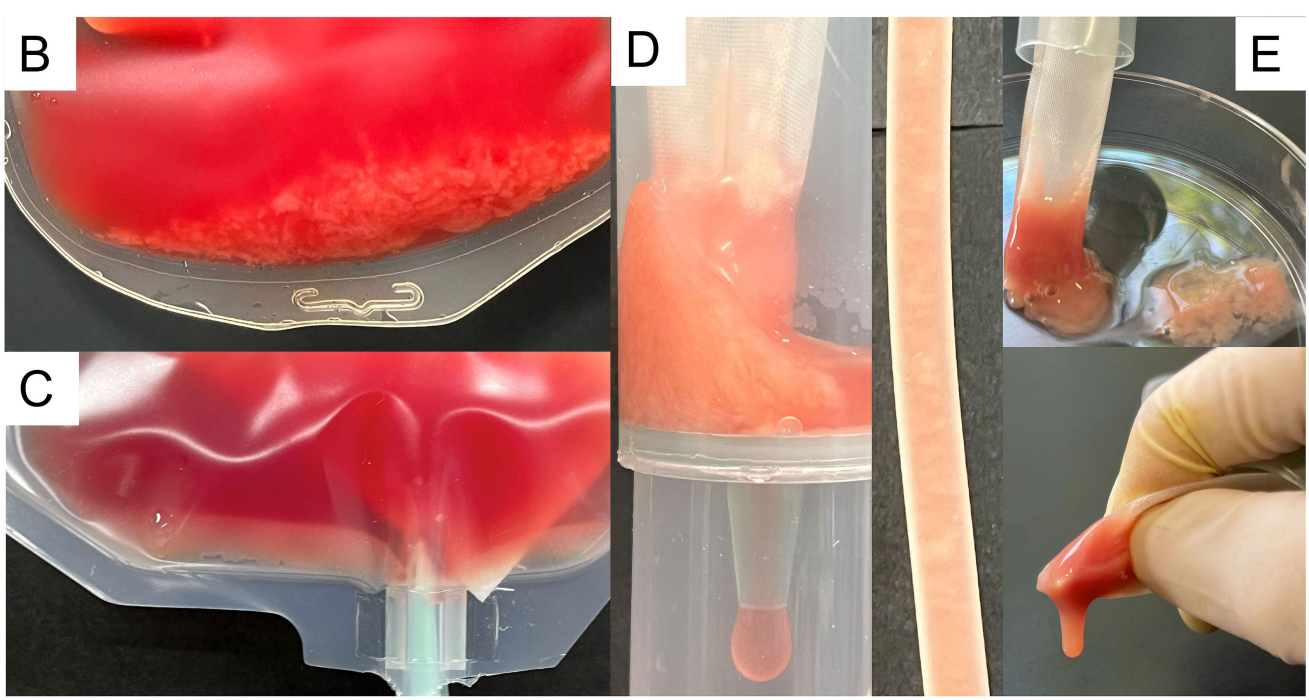
B
C
D
E

Figure 2.

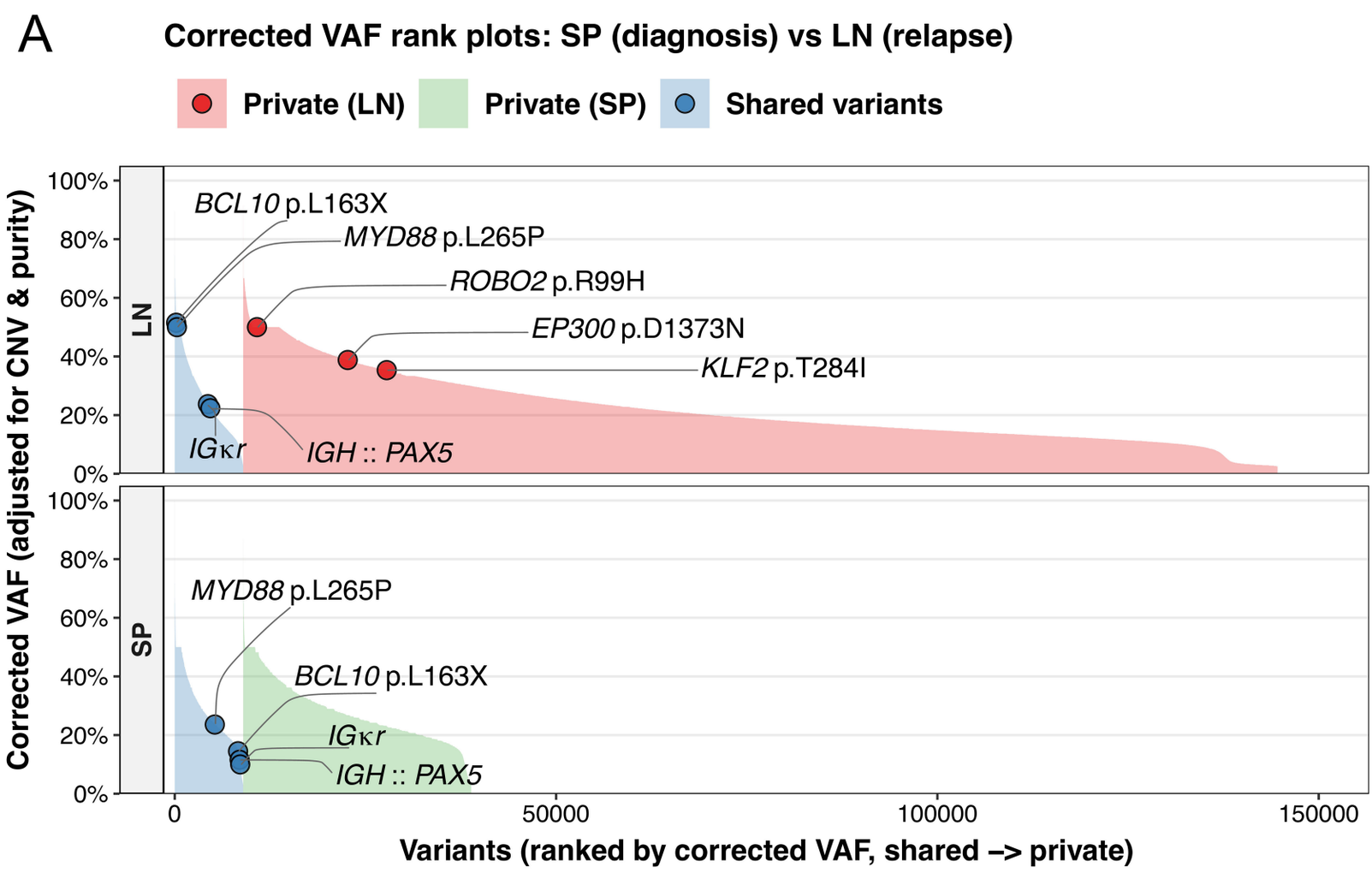
A
Corrected VAF rank plots: SP (diagnosis) vs LN (relapse)
Private (LN)
Private (SP)
Shared variants
Corrected VAF (adjusted for CNV & purity)
LN
SP
BCL10 p.L163X
MYD88 p.L265P
ROBO2 p.R99H
EP300 p.D1373N
KLF2 p.T284I
IGκr
IGH :: PAX5
100%
80%
60%
40%
20%
0%
0
50000
100000
150000
Variants (ranked by corrected VAF, shared –> private)

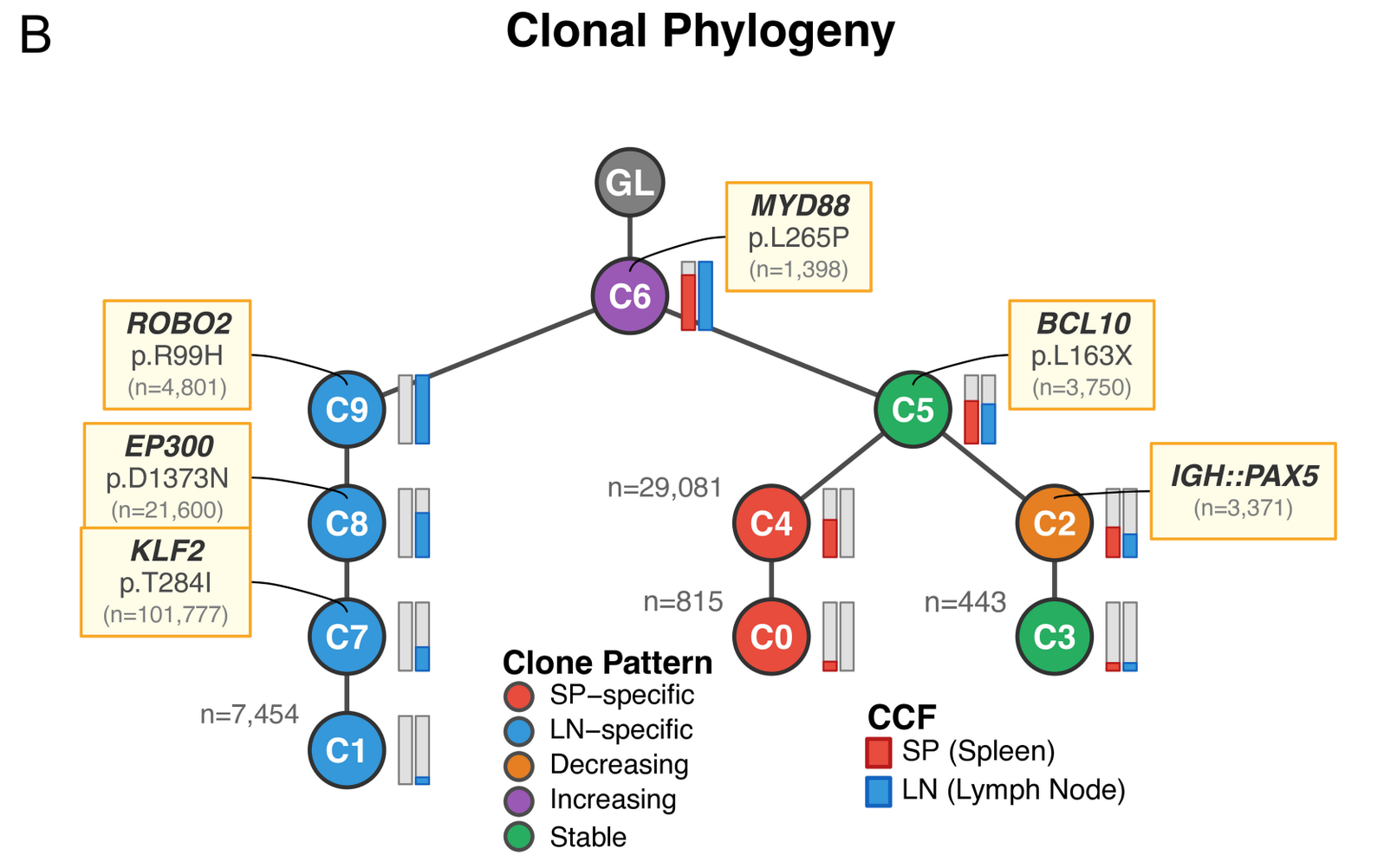
B
Clonal Phylogeny
GL
C6
MYD88
p.L265P
(n=1,398)
ROBO2
p.R99H
(n=4,801)
C9
EP300
p.D1373N
(n=21,600)
C8
KLF2
p.T284I
(n=101,777)
C7
n=7,454
C1
C5
BCL10
p.L163X
(n=3,750)
n=29,081
C4
n=815
C0
C2
IGH::PAX5
(n=3,371)
n=443
C3
Clone Pattern
SP–specific
LN–specific
Decreasing
Increasing
Stable
CCF
SP (Spleen)
LN (Lymph Node)